

# Dehydration Studies of a High-Surface-Area Alumina (Pseudo-boehmite) Using Solid-State $^1\text{H}$ and $^{27}\text{Al}$ NMR

John J. Fitzgerald,<sup>\*,†</sup> Gilberto Piedra,<sup>†</sup> Steven F. Dec,<sup>‡</sup> Mark Seger,<sup>‡</sup> and Gary E. Maciel<sup>\*,‡</sup>

Contribution from the Departments of Chemistry, South Dakota State University, Brookings, South Dakota 57007, and Colorado State University, Fort Collins, Colorado 80523

Received March 11, 1997. Revised Manuscript Received May 27, 1997<sup>⊗</sup>

**Abstract:**  $^1\text{H}$  NMR based on the CRAMPS technique has been used to identify and monitor the protons of surface Al–OH groups and “physisorbed” water associated with a high-surface-area (230 m<sup>2</sup>/g) pseudo-boehmite material following dehydration in the 110–1100 °C temperature range. Three distinguishable  $^1\text{H}$  CRAMPS peaks were identified: a broad peak at  $4.0 \pm 0.2$  ppm attributed to the protons of “physisorbed” water and two peaks at  $8.2 \pm 0.3$  and  $2.3 \pm 0.2$  ppm associated with the protons of structural Al–OH groups. The  $^1\text{H}$  CRAMPS results are interpreted in relationship to two important regions of the experimental dehydration weight-loss profile for this material, a lower temperature region (110–300 °C), in which desorption of “physisorbed” water occurs, and an intermediate temperature region (350–550 °C), where condensation of adjacent Al–OH groups occurs. The combination of heating between 110 and 300 °C and room temperature evacuation were found to eliminate the “physisorbed” water peak, permitting the observation of the two resonances associated with the structural Al–OH sites. Dipolar dephasing experiments indicate that the 8.2 ppm peak is associated with highly coupled, “clustered” Al<sub>2</sub>OH groups, while the 3.0 ppm resonance is associated with terminal, “isolated” AlOH groups.  $^1\text{H}$  CRAMPS evidence shows that upon heat treatment the Al<sub>2</sub>OH groups condense at lower temperatures (350 °C) than the AlOH groups (550 °C). Three mechanisms are proposed for the condensation of the proton-containing surface Al–OH groups that occur in this material, based on crystalline boehmite as a structural model. In addition to  $^1\text{H}$  CRAMPS studies,  $^{27}\text{Al}$  MAS NMR spectra at 14 T of samples dehydrated from 100 to 1100 °C provide structural information about the aluminums in the high-surface-area pseudo-boehmite. This material dehydrates by condensation of both Al<sub>2</sub>OH and AlOH groups to form distorted, hydrogen-bearing 4-, 5-, and 6-coordinate aluminum-containing intermediates in the 350–500 °C range. At 1100 °C, this hydrogen-bearing  $\gamma$ - or  $\delta$ -alumina material is converted to a material consisting of primarily  $\alpha$ -Al<sub>2</sub>O<sub>3</sub>.

## Introduction

Alumina-based materials are widely used as catalysts, catalyst supports, adsorbents, coatings, ceramics, and abrasives.<sup>1–3</sup> The state of hydration of a specific alumina material is related to its stoichiometry and structure. Various aluminum oxide-based materials of importance include the anhydrous and hydrous aluminum oxides and hydroxides and a wide range of calcined, aluminum oxides such as corundum or  $\alpha$ -alumina ( $\alpha$ -Al<sub>2</sub>O<sub>3</sub>),  $\gamma$ -alumina, and transitional aluminas.<sup>1</sup> The hydroxides gibbsite and bayerite have related crystal structures,<sup>1–3</sup> with double layers of a hexagonal closely packed array of hydroxyl ions; each aluminum is coordinated to six anions that form edge-shared octahedral Al(OH)<sub>6</sub> structural units. The double layers in gibbsite are stacked in the direction of the *c* axis with repeating A and B layers of the sequence ABBAABBA, while in bayerite,<sup>2</sup> the stacking arrangement is ABABAB, with the double layers held together by hydrogen bonds between adjacent hydroxyl ions.

Aluminum oxyhydroxide [AlO(OH)] occurs in two distinct forms, boehmite and diaspora, that exist in a hexagonal closed-packed arrangement of hydrogen-bonded oxides built up of edge-sharing AlO<sub>4</sub>(OH)<sub>2</sub> or AlO<sub>3</sub>(OH)<sub>3</sub> octahedral units.<sup>4</sup> Di-

aspore contains two types of Al–O bonding interactions; one oxygen is approximately coplanar with the three surrounding aluminums, and the second oxygen forms a pyramid with the three adjacent aluminums. In boehmite, the Al<sup>3+</sup> ion exists in a distorted, edge-sharing octahedral array of oxide ions that forms a double layer, with the layers being connected by zigzag chains of hydrogen bonds.<sup>5</sup> Pseudo-boehmite is a poorly crystallized boehmite with a water content of 1.5–2.5 mol.<sup>4</sup> The XRD pattern of pseudo-boehmite shows broad lines that coincide with that of boehmite.<sup>1</sup>

The transitional aluminas,  $\chi$ -Al<sub>2</sub>O<sub>3</sub>,  $\eta$ -Al<sub>2</sub>O<sub>3</sub>,  $\gamma$ -Al<sub>2</sub>O<sub>3</sub>,  $\kappa$ -Al<sub>2</sub>O<sub>3</sub>, and  $\theta$ -Al<sub>2</sub>O<sub>3</sub>, are formed from oxyhydroxides and hydroxides under various dehydration or dehydroxylation conditions, where these two terms represent the formal loss of water by desorption of “physisorbed” water or by condensation of hydroxyl groups, respectively.<sup>1,3,4</sup> The materials,  $\gamma$ -Al<sub>2</sub>O<sub>3</sub> and  $\eta$ -Al<sub>2</sub>O<sub>3</sub>, crystallize in a defect spinel structure, with  $\eta$ -Al<sub>2</sub>O<sub>3</sub> being a more effective acidic catalyst than  $\gamma$ -Al<sub>2</sub>O<sub>3</sub> for olefin isomerization reactions.<sup>4</sup> Strongly dried aluminas chemisorb at least a monolayer of water when exposed to moisture at room temperature.<sup>5</sup> According to De Boer et al.,<sup>6</sup> the hydration surface of  $\gamma$ -alumina retains 13 molecules of water/100 Å<sup>2</sup> of surface after evacuation at 25 °C for 100 h, while after drying at 120 °C,  $\gamma$ -Al<sub>2</sub>O<sub>3</sub> still retains 8.25 molecules of water/100 Å<sup>2</sup>.<sup>6</sup> Peri and Hannan<sup>7</sup> found that  $\gamma$ -alumina adsorbs water at room temperature and after calcina-

\* To whom correspondence should be addressed.

† South Dakota State University.

‡ Colorado State University.

⊗ Abstract published in *Advance ACS Abstracts*, August 1, 1997.

(1) Wefers, K.; Misra, C. *Oxides and Hydroxides of Aluminum*; Alcoa Technical Paper No. 19, Alcoa Laboratories, 1987.

(2) Gitzen, W. H. *Alumina as a Ceramic Material*; The American Ceramic Society: Columbus, OH, p 15.

(3) Walter, T. H.; Oldfield, E. *J. Phys. Chem.* **1989**, *93*, 6744–6752.

(4) Cocke, D. L.; Johnson, E. D.; Merrill, R. P. *Catal. Rev.—Sci. Eng.* **1984**, *26*, 163–231.

(5) Peri, J. B. *J. Phys. Chem.* **1965**, *69*, 211–219.

(6) DeBoer, J. H.; Fortuin, J. M. H.; Lippens, B. C.; Meijs, W. H. *J. Catalysis* **1963**, *2*, 1–7.

(7) Peri, J. B.; Hannan, R. B. *J. Phys. Chem.* **1960**, *64*, 1526–1530.

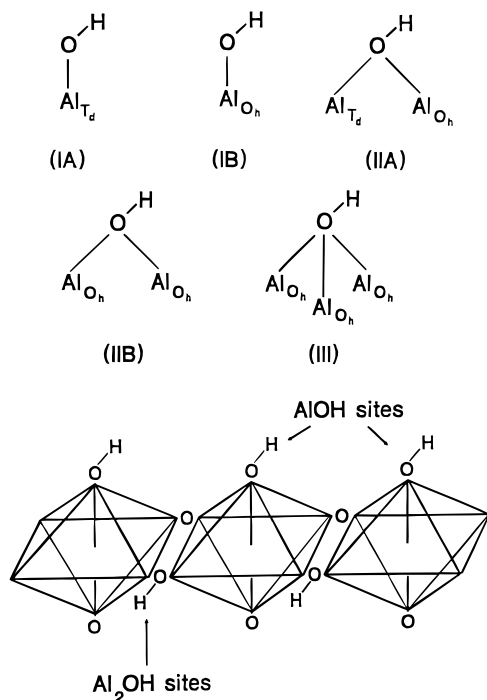
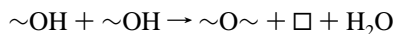


**Figure 1.** (a) Types of surface hydroxyl groups of  $\gamma$ -alumina, as proposed by Peri.<sup>9</sup> (b) Two types of structural hydroxyl sites of boehmite.

tion at 600 °C and reexposure to moist air. The adsorbed water is believed to exist in the forms of both “physisorbed” water and surface hydroxyl groups. At lower temperature heating, desorbed water molecules react to form “surface” hydroxyl groups; at higher temperatures, the adjacent surface hydroxyls condense to form water molecules, which are subsequently removed by evacuation according to the dehydration reaction



where  $\square$  represents an oxide vacancy<sup>8</sup> for 4- or 5-coordinated  $\text{AlO}_x$  sites formed from 6-coordinate sites. From infrared studies, Peri<sup>6</sup> and Knözinger and Ratnasamy<sup>7</sup> postulated a surface model for  $\gamma$ -alumina that includes the five different surface hydroxyl sites shown in Figure 1, thus providing a framework for discussing and describing the various proton, oxygen, and aluminum atoms associated with the surface  $\text{Al}-\text{OH}$  sites. In terms of this model, aluminum oxyhydroxides and transitional aluminas contain at least one of the five distinct hydroxyl sites, with the Type III site being the most acidic and Types IA and IB the most basic.<sup>5</sup>

Solid-state NMR techniques provide unique capabilities to obtain information about both the structural nature and dynamics of the surface chemistry of alumina materials. Morris and Ellis<sup>13</sup> used solid-state  $^{27}\text{Al}$  CP/MAS NMR to study the surfaces of various  $\gamma$ -aluminas.  $^{27}\text{Al}$  CP/MAS NMR spectra of  $\gamma$ -alumina showed peaks at 6.0 and 55 ppm due to octahedral and tetrahedral  $\text{Al}-\text{OH}$  surface sites, while calcination to different degrees of dehydroxylation broadened the  $^{27}\text{Al}$  NMR signal at 6 ppm. Heating to 815 °C resulted in a complete loss of the

NMR signal due to the removal of adjacent hydroxyl groups.<sup>13</sup> The  $^{27}\text{Al}$  CP/MAS NMR spectrum of partially dehydroxylated  $\gamma$ -alumina showed peaks due to surface 4- and 6-coordinated  $\text{Al}-\text{OH}$  Brönsted sites.<sup>13</sup> Huggins and Ellis<sup>14</sup> also carried out variable-temperature  $^{27}\text{Al}$  MAS NMR studies to examine the surfaces of transition aluminas. They proposed an alumina surface model based on three mechanisms of surface dynamics: (1) two neighboring hydroxyl groups condense, with formation of molecular water that may move or “hop” across the surface, leave the surface, reassociate to form two adjacent hydroxyls or cap a Lewis acid site ( $\text{AlO}_5$ ); (2) surface proton movement causes rearrangement of hydroxyl groups to new positions; and (3) the Lewis sites migrate and the hydroxyl groups move. The first mechanism occurs on untreated aluminas with large concentrations of hydroxyl groups, whereas the later mechanisms occur on alumina surfaces with or without “physisorbed” water. Coster, Blumenfeld, and Fripiat<sup>15</sup> recently used  $^1\text{H}-^{27}\text{Al}$  CP/MAS NMR to examine Lewis acidity in pretreated aluminas. Isotopically enriched  $^{15}\text{NH}_3$  was used to probe the surface sites by magnetization transfer from  $\text{NH}_3$  to surface aluminas. Two types of surface Lewis acid sites were observed for chemisorption of  $\text{NH}_3$ : a 4-coordinate peak at 58 ppm and a 5-coordinate site at 40 ppm. Chemisorption of water by rehydration converted these sites to 5-coordinate and 6-coordinate sites, respectively.

Walter and Oldfield<sup>3</sup> reported  $^{17}\text{O}$  CP/MAS NMR of bulk and surface sites on aluminum oxides and transitional aluminas. The  $^{17}\text{O}$  NMR of  $^{17}\text{O}$ -enriched boehmite revealed two peaks assigned to  $\text{OAl}_4$  and  $\text{Al}_2\text{OH}$  sites, while  $^1\text{H}-^{17}\text{O}$  cross polarization (CP) selectively enhanced the weak  $\text{Al}_2\text{OH}$  signal. Transition aluminas contained two types of oxygen sites: tetrahedral  $\text{OAl}_3$  and, to a lesser extent, trigonal  $\text{OAl}_3$ .<sup>3</sup> The range of bond angles and bond distances for the trigonal sites is due to a range of  $^{17}\text{O}$  chemical shifts and quadrupole coupling constants.

While extensive solid-state  $^1\text{H}$  CRAMPS studies have not been reported for alumina materials, this approach offers a direct means to explore the surface proton population on alumina materials. Bronnimann et al.<sup>16,17</sup> used  $^1\text{H}$  CRAMPS techniques to explore the surfaces of silica-aluminas,  $\gamma$ -alumina, and silica gel. For alumina-silicas, a sharp 2.0 ppm peak was assigned to  $\text{Si}-\text{OH}$  groups, while two broad peaks at 3.1 and 4.8 ppm were assigned to water “physisorbed” onto silica-like regions and to  $\gamma$ -alumina-like regions, respectively. The peak at 7 ppm was attributed to bridged Brönsted sites, although Pfeifer et al.<sup>18</sup> assigned it to residual ammonium species.

The present work summarizes  $^1\text{H}$  CRAMPS NMR investigations to examine the hydroxyl groups and “physisorbed” water moieties on a high-surface-area (230  $\text{m}^2/\text{g}$ ) pseudo-boehmite ( $\text{Al}_2\text{O}_3 \cdot 2.05\text{H}_2\text{O}$ ) material following various dehydration treatments. This report describes the relationship between the  $^1\text{H}$  CRAMPS spectra of this material and its experimental weight-loss profiles, following low-temperature dehydration (50–110 °C) and higher temperature dehydroxylation (300–1100 °C) under ambient pressure and in vacuo conditions.  $^{27}\text{Al}$  NMR spectra are also reported for pseudo-boehmite materials dehy-

(14) Huggins, B. A.; Ellis, P. D. *J. Am. Chem. Soc.* **1992**, *114*, 2098–2108.

(15) Coster, D.; Blumenfeld, A. L.; Fripiat, J. J. *J. Phys. Chem.* **1994**, *98*, 6201–6211.

(16) Bronnimann, C. E.; Chuang, I.; Hawkins, B. L.; Maciel, G. E. *J. Am. Chem. Soc.* **1987**, *109*, 1562–1564.

(17) Bronnimann, C. E.; Zeigler, R. C.; Maciel, G. E. *J. Am. Chem. Soc.* **1988**, *110*, 2023–2026.

(18) Pfeifer, H. Applications of NMR Spectroscopy to Surfaces and Catalysts: Acidic Sites and Adsorbed Species. In *Nuclear Magnetic Resonance in Modern Technology*; Maciel, G. E., Ed.; NATO ASI Series, Vol. 447; Kluwer Academic Publishers: Dordrecht, The Netherlands, 1994; p 504.

(8) Gates, B. C.; Katzer, J. R.; Schuit, G. C. A. *Chemistry of Catalytic Processes*; McGraw-Hill: New York, 1979; pp 249–260.

(9) Peri, J. B. *J. Phys. Chem.* **1965**, *69*, 220–230.

(10) Knözinger, H.; Ratnasamy, P. *Catal. Rev.—Sci. Eng.* **1978**, *17*, 31–70.

(11) Parkyns, N. D. *J. Phys. Chem.* **1971**, *75*, 526–531.

(12) Peri, J. B. *J. Phys. Chem.* **1965**, *69*, 231–239.

(13) Morris, H. D.; Ellis, P. D. *J. Am. Chem. Soc.* **1989**, *111*, 6045–6049.

drated from 100 to 1100 °C to obtain NMR information on local structural aluminum site changes. These changes have been related to changes in the proton populations obtained from the  $^1\text{H}$  CRAMPS results.

## Experimental Section

$^1\text{H}$  CRAMPS experiments were taken at 187 and 360 MHz on modified Nicolet NT-200 and NT-360 spectrometers, using the BR-24 pulse sequence<sup>20</sup> and "home-built" probes, of samples sealed under vacuum in thick-walled 5 mm (OD) glass tubes (Wilmad PS241), following evacuation at 6.5 mTorr for 24 h, unless otherwise specified. The sealed NMR tubes were spun with a spinning system based on a modification of a design by Gay<sup>19</sup> at MAS speeds of 1.2–1.5 kHz. The 187 MHz CRAMPS spectra were obtained with ( $\tau$ ) spacings of 3.0 and 1.2  $\mu\text{s}$   $\pi/2$  pulses. The 360 MHz CRAMPS spectra were obtained with  $\tau \approx 3.1$  and 1.4  $\mu\text{s}$   $\pi/2$  pulses. All spectra were referred to the chemical shift of tetrakis(trimethylsilyl)silane (TTMSS) at 0.38 ppm via sample substitution (with liquid tetramethylsilane at 0.00 ppm).

$^{27}\text{Al}$  NMR spectra were recorded on a Bruker AM-600 spectrometer, using home-built probes or a Chemagnetics Infinity 600 spectrometer, using 3.2 and 4.0 mm Chemagnetics MAS systems, with evacuated samples that were loaded into the spinner in a drybox. To ensure minimum error in the quantitation of the observed NMR peak intensities, short excitation pulses (<22° tip angles) were used. MAS speeds of 16–17 kHz were employed. The chemical shift reference was an aqueous solution of 1 M  $\text{AlCl}_3 \cdot 6\text{H}_2\text{O}$ , assigned a chemical shift of 0.0 ppm. Higher chemical shifts correspond to larger resonance frequencies and lower shielding constants. For  $^{27}\text{Al}$  spin counting experiments, based on a previously reported method,<sup>39</sup> the spinning angle was set approximately 1° off the magic angle to broaden into the baseline the extensive spinning sideband arrays due to the noncentral transitions. This facilitated integration of the centerband signal as a function of the pulse width in this single-pulse experiment. An authentic sample of kaolin of known water content served as a spin counting standard.

(19) Gay, I. D. *J. Magn. Reson.* **1984**, *58*, 413.

(20) Burum, D. P.; Rhim, W. K. *J. Phys. Chem.* **1979**, *71*, 944–956.

(21) Christoph, G. G.; Corbató, C. E.; Hofmann, D. A.; Tettenhorst, R. T. *Clay Clay Miner.* **1979**, *27*, 81–86.

(22) Hill, R. J. *Clay Clay Miner.* **1981**, *29*, 435–445.

(23) Christensen, A. N.; Lehman, M. S.; Convert, P. *Acta Chem. Scand.* **1982**, *A36*, 303–308.

(24) Corbató, C. E.; Tettenhorst, R. T.; Christoph, G. G. *Clay Clay Miner.* **1985**, *33*, 71–75.

(25) Haase, J.; Freude, D.; Frlich, T.; Himpel, G.; Kerbe, F.; Lippmaa, E.; Pfeifer, H.; Sarv, P.; Schfer, H.; Seiffert, B. *Chem. Phys. Lett.* **1989**, *156*, 328–332.

(26) John, C. S.; Alma, N. C.; Hays, G. R. *Appl. Catal.* **1982**, *6*, 341–346.

(27) Dec, S. F.; Maciel, G. E.; Fitzgerald, J. J. *J. Am. Chem. Soc.* **1990**, *112*, 9069–9077.

(28) Fitzgerald, J. J.; Dec, S. F.; Hamza, A. I. *Am. Mineral.* **1989**, *74*, 1405–1408.

(29) Lambert, S. F.; Millman, W. S.; Fripiat, J. *J. Am. Chem. Soc.* **1989**, *111*, 3517–3522.

(30) Cruickshank, M. C.; Dent Glasser, L. S.; Barri, A. I.; Pople, I. J. *J. Chem. Soc., Chem. Commun.* **1986**, 23–24. Alemany, L. B.; Kirker, G. W. *J. Am. Chem. Soc.* **1986**, *108*, 6158–6162.

(31) Dec, S. F.; Fitzgerald, J. J.; Frye, J. S.; Shatlock, M. P.; Maciel, G. E. *J. Magn. Reson.* **1991**, *93*, 403–406.

(32) Gilson, J.-P.; Edwards, G. C.; Peters, A. W.; Rajagopalan, K.; Wormsbecker, R. F.; Roberie, T. G.; Shatlock, M. P. *J. Chem. Soc., Chem. Commun.* **1987**, 91–92.

(33) Lippens, B. C.; de Boer, J. H. *Acta Crystallogr.* **1964**, *17*, 1312–1321.

(34) O'Reilly, D. E. *Adv. Catal.* **1960**, *12*, 31.

(35) Pearson, R. M.; Schramm, C. M. *Colloids Surf.* **1990**, *45*, 323–334 and references therein.

(36) Haase, J.; Oldfield, E. *J. Magn. Reson. A* **1993**, *104*, 1–9.

(37) Schmitt, K. D.; Haase, J.; Oldfield, E. *Zeolites* **1994**, *14*, 89–100.

(38) Maciel, G. E.; Bronnimann, C. E.; Hawkins, B. L. High-Resolution  $^1\text{H}$  Nuclear Magnetic Resonance in Solids by CRAMPS. In *Advances in Magnetic Resonance*; The Waugh Symposium, Vol. 14; Warren, S., Ed.; Academic Press: San Diego, CA, 1990; pp 125–150.

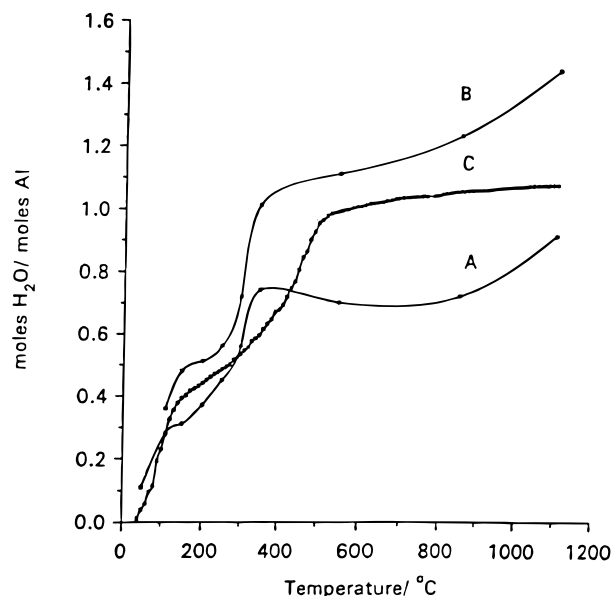


**Figure 2.** Weight-loss profiles for the high-surface-area pseudo-boehmite ( $\text{Al}_2\text{O}_3 \cdot 2.05\text{H}_2\text{O}$ ) material. (a) Gravimetric analysis of samples equilibrated in aqueous suspensions over the pH range 3–12 (curve A). (b) Gravimetric analysis of "as received" samples (curve B). (c) Thermogravimetric (TGA) analysis of an "as received" sample in ambient atmosphere at 20 °C/min (curve C).

## Results and Discussion

### Experimental Weight-Loss Data For High-Surface-Area Pseudo-boehmite.

The high-surface-area (HSA) pseudo-boehmite was obtained from Norton (lot 08061, surface area 230  $\text{m}^2/\text{g}$ , average particle size 46  $\mu\text{m}$ , and pore volume > 0.5  $\text{mL}/\text{g}$ ). Three series of pseudo-boehmite samples were prepared in order to obtain the weight loss at various heating temperatures (weight-loss profiles), as given in Figure 2. In the experiments represented in curve A, high-surface-area pseudo-boehmite samples were suspended in 0.02 M NaCl for 1 h, followed by equilibration in aqueous solutions at pH 3.0, 5.0, 6.5, 7.5, 9.0, 11.0, and 12.0 solutions for 24 h. Adjustment of the pH was carried out by addition of either 1.0 M HCl or 1.0 M NaOH solutions. The resulting solid materials obtained from the slurries were pressure filtered under 95 psi of  $\text{N}_2$ , using a Gelman pressure filtration funnel with a 45  $\mu\text{m}$  Nylaflo nylon membrane filter. Following desiccation over Drierite for 72 h at atmospheric pressure (725 Torr), the solids were heated at atmosphere pressure in the temperature range 110–1100 °C until a constant weight was obtained. A weight-loss profile was obtained by plotting the average weight loss of these materials at the various temperatures (50, 110, 150, 200, 250, 300, 350, 550, 850, and 1100 °C) versus the heating temperature (curve A, Figure 2).

In the experiments represented in curve B, the effects of dehydration/dehydroxylation were examined on samples prepared from "as received" material by heating the samples at ambient pressure at the same temperatures and during the same periods of time indicated above for the samples related to curve A. A weight-loss profile was also obtained as shown in curve B of Figure 2.

In the work represented in curve C, two TGA thermograms were obtained (from Hazen Research Inc. in Golden, CO) on a "as received" pseudo-boehmite sample heated in ambient atmosphere ( $\sim 725$  Torr) at 20 °C/min to a limit of 1100 °C and on an analogous sample heated to 1100 °C at 20 °C/min under 152 Torr vacuum. The TGA thermogram obtained in ambient atmosphere is shown as curve C of Figure 2, which is

**Table 1.** Average Weight Losses (as mol of water/mol of Al)

temp, °C	weight loss as %wt			weight loss as H <sub>2</sub> O/mol of Al <sup>d</sup>		
	SE <sup>a</sup>	AR <sup>b</sup>	TGA <sup>c</sup>	SE <sup>a</sup>	AR <sup>b</sup>	TGA <sup>c</sup>
50	3		1	0.11		0.04
110	4	9	7	0.28	0.36	0.29
150	8	11	10	0.31	0.42	0.40
200	10	13	12	0.37	0.51	0.44
250	12	15	13	0.45	0.56	0.50
300	15	19	14	0.56	0.72	0.54
350	19	26	16	0.74	1.01	0.60
550	18	29	26	0.70	1.11	0.99
850	20	32	27	0.72	1.23	1.06
1100	24	38	28	0.91	1.44	1.08

<sup>a</sup> Solution-equilibrated material, corresponds to curve A in Figure 2. <sup>b</sup> "As received" material, corresponds to curve B in Figure 2. <sup>c</sup> Thermogravimetric analysis, corresponds to curve C in Figure 2. <sup>d</sup> Maximum moles of water in 2.05.

virtually identical with the profile for the sample dehydrated under vacuum.

In this article, unless different conditions are specified explicitly, the term "dehydrated" or "heated" signifies heating the sample at ambient pressure (~725 Torr), and the term "evacuated" or "evacuation" signifies subjecting the sample to some specified vacuum (or 6.5 mTorr, if not otherwise specified), at room temperature.

#### Weight-Loss Profiles for Dehydration/Dehydroxylation.

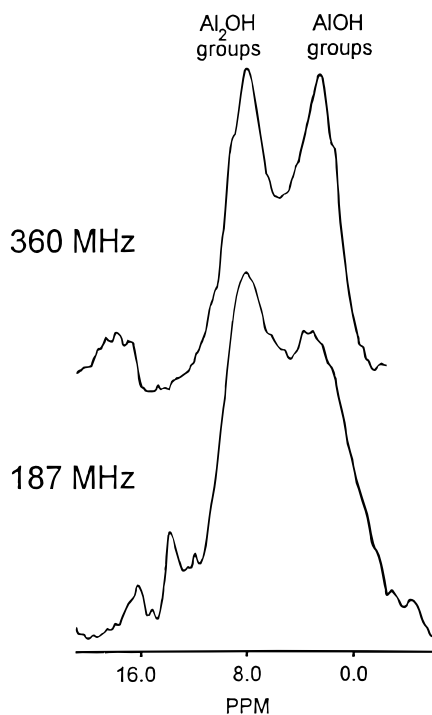
Two processes have been postulated<sup>5</sup> to occur during the dehydration of alumina materials: (1) loss of water molecules by desorption of physically adsorbed or bulk molecular water and (2) condensation of adjacent surface or internal hydroxyl groups. Both processes are associated with the weight-loss profiles observed upon heating alumina materials. The desorption of "physisorbed" water has been postulated to occur at lower temperatures (100–120 °C),<sup>6</sup> while condensation of hydroxyl groups occurs above 110 °C. Removal of hydroxyl groups during water condensation conditions has been postulated to give rise to strained Al–O–Al linkages on the alumina surface, imparting catalytic properties to the alumina materials. Since the pseudo-boehmite material is composed exclusively of octahedral AlO<sub>6</sub> sites (Figure 1b), it is possible that the oxygen vacancies produced during the condensation of hydroxyl groups reduce the aluminum coordination number to 5, thereby forming Lewis acid AlO<sub>5</sub> structural moieties.

Table 1 summarizes the average gravimetric weight losses of solution-equilibrated and "as received" solid samples of a pseudo-boehmite material (Norton, Al<sub>2</sub>O<sub>3</sub>·2.05H<sub>2</sub>O) heated at various temperatures from 50 to 1100 °C at ambient pressure. Some weight-loss data obtained from the TGA thermogram obtained in ambient atmosphere are also included in Table 1 for comparison. The weight-loss profiles, plotted as mol of H<sub>2</sub>O/mol of Al (maximum equals 2.05 H<sub>2</sub>O/Al) versus dehydration/dehydroxylation temperature, for the various high-surface-area alumina materials studied are given in Figure 2. Curve A shows the average weight loss for the series of samples equilibrated in aqueous solutions with pHs ranging from 3.0 to 12.0. This gravimetric weight-loss curve shows three distinguishable regions: (1) an initial region of weight loss from 50 to 200 °C corresponding to a dehydration process that can be related to the removal of "physisorbed" and/or bulk molecular water prior to the condensation of hydroxyl groups on the alumina material, (2) a temperature region from 200 to 350 °C, in which significant weight-loss is observed that is associated with the first stage of dehydration by condensation of Al–OH groups, and (3) a final region of weight loss in the 350–1100 °C temperature range that is attributed to a second stage of dehydration by condensation of hydroxyl groups.

Figure 2 also shows the weight-loss profile for "as received" samples of high-surface-area alumina obtained by gravimetric analysis (curve B) and by thermogravimetric analysis (curve C), in the same temperature range (50–1100 °C). Curve B corresponds to the average gravimetric weight-loss profile and depicts three regions: (1) an initial region from 110 to 200 °C associated with the removal of "physisorbed" water, (2) a second region in the 200–350 °C temperature range where a sharp increase in the weight loss is observed, attributed to dehydration via the condensation of hydroxyl groups, and (3) a final region from 350 to 1100 °C, showing further dehydration/condensation behavior similar to that observed in the final region of curve A. The TGA thermogram of the "as received" samples heated at 20 °C/min in ambient atmosphere (curve C) also depicts three regions: (1) an initial low-temperature region (50–150 °C) in which a sharp increase in weight loss occurs due to the removal of "physisorbed" and bulk molecular water, (2) a second region in the 150–500 °C range that is associated with dehydration due to condensation of hydroxyl groups, and (3) a third dehydration/dehydroxylation region (500–1100 °C), probably due to additional dehydration by condensation of hydroxyl groups, where the weight-loss increases only slightly. The TGA thermogram for the "as received" sample heated at 20 °C/min in vacuo shows results (not shown) similar to those obtained for the "as received" sample heated at 20 °C/min in ambient atmosphere (curve C).

Both the gravimetric curves (A and B) and TGA curve (C) are comparable at low temperature during the first dehydration stages, where the desorption of "physisorbed" water occurs; however, at high temperatures, the weight-loss profile derived from the gravimetric measurements for the solution-equilibrated material is less steep than the weight-loss profiles derived from both the gravimetric and TGA measurements with "as received" materials. The lower weight-loss values observed for the solution-equilibrated materials may be due to readsorption of the water onto the alumina material following cooling to room temperature. The weight-loss values obtained for samples from the TGA analysis are intermediate between the two sets of gravimetric measurements. In the TGA analysis, the alumina sample is systematically heated from 50 to 1100 °C under conditions that do not permit water readsorption, but the heating time period is much shorter than that utilized in the gravimetric measurements (a minimum of 24 h). The gravimetric measurements with the "as received" samples show the highest weight-loss values, probably due to the longer time periods of heating at these temperatures.

**<sup>1</sup>H CRAMPS NMR Results.** The <sup>1</sup>H CRAMPS spectra, obtained at frequencies of 187 and 360 MHz, on the high-surface-area alumina sample equilibrated at pH 6.5, then heated at 110 °C at ambient pressure, and then evacuated at 6.5 mTorr at 25 °C for 24 h, are shown in Figure 3. The two resonances centered at ca. 3.0 and 8.2 ppm are tentatively assigned on the basis of patterns observed in this work (vide infra) to two distinguishable structural Al–OH bulk moieties, an octahedral AlOH site and an octahedral Al<sub>2</sub>OH site, respectively, as depicted in Figure 1b. These two different types of structural Al–OH groups may be either internal or external groups, based on the microporous nature of this material (vide infra). These two 6-coordinate aluminum sites of the pseudo-boehmite material are probably similar to the Type IB and Type IIB sites of the surface model proposed by Peri<sup>9,10</sup> for  $\gamma$ -alumina, as shown in Figure 1a. These two types of Al–OH sites are known to exist in crystalline boehmite in a 1:1 ratio based on its crystal structure, as shown in Figure 1b.<sup>21–24</sup> The <sup>1</sup>H CRAMPS results show that an increase in the magnetic field from 4.39 to 8.45 T



**Figure 3.**  $^1\text{H}$  CRAMPS NMR spectra (187 and 360 MHz) of a pseudo-boehmite ( $\text{Al}_2\text{O}_3 \cdot 2.05\text{H}_2\text{O}$ ) material equilibrated in an aqueous suspension at pH 6.5, filtered, heated at  $110^\circ\text{C}$  for 5 h, and evacuated for 24 h at 6.5 mTorr.

increases the resolution of the proton peaks, probably because of a narrowing of the observed resonances as a result of decreased quadrupolar interference with MAS averaging of the  $^1\text{H}$ – $^{27}\text{Al}$  dipolar interactions.<sup>25</sup> The presence of two aluminums close to the protons in the  $\text{Al}_2\text{OH}$  sites should be expected to cause the proton peak of the  $\text{Al}_2\text{OH}$  group to be broader than that of the corresponding proton peak of the  $\text{Al}-\text{OH}$ ; however, the chemical shift dispersion due to a wide range of different proton environments in both the  $\text{AlOH}$  and  $\text{Al}_2\text{OH}$  sites is probably the dominant line broadening influence at higher fields, e.g., 360 MHz.

The 360 MHz  $^1\text{H}$  CRAMPS NMR spectra (not given here) for pseudo-boehmite materials equilibrated in aqueous suspensions at various pH values (3.0, 6.5, and 12.0), followed by simultaneous heating and evacuation at  $110^\circ\text{C}$  and at 6.5 mTorr show two peaks centered at 8.2 and 3.0 ppm similar to those of Figure 3 associated with structural  $\text{Al}_2\text{OH}$  and  $\text{AlOH}$  sites, respectively. The relative intensity of the 3.0 ppm peak is drastically decreased at the lower pH of 3.0, probably due to the protonation of  $\text{AlOH}$  sites with concomitant formation of surface  $\text{Al}(\text{III})-\text{OH}_2$  species. These protonated species would account for the presence of a peak at about 4.0 ppm associated with water molecules (*vide infra*) physically adsorbed onto the pseudo-boehmite material. Higher pH values did not drastically change the population of either  $\text{Al}_2\text{OH}$  or  $\text{AlOH}$  sites on the pseudo-boehmite material, although it seems that at the very high pH values the number of  $\text{Al}_2\text{OH}$  sites is increased.

$^1\text{H}$ – $^1\text{H}$  dipolar dephasing experiments of the type described previously<sup>16</sup> for the study of silica gel to qualitatively determine the relative strengths of the  $^1\text{H}$ – $^1\text{H}$  dipolar coupling between protons of the two types of silanols on silica were used here. The  $^1\text{H}$  CRAMPS dipolar dephasing results obtained with dephasing times from 0 to  $80\ \mu\text{s}$  are shown in Figure 4 for the alumina sample that was heated at ambient pressure  $110^\circ\text{C}$ , followed by evacuation at 6.5 mTorr for at  $25^\circ\text{C}$  24 h. These results show that the resonance at 8.2 ppm is dephased beyond observation after a dephasing time of  $20\ \mu\text{s}$ , whereas the peak

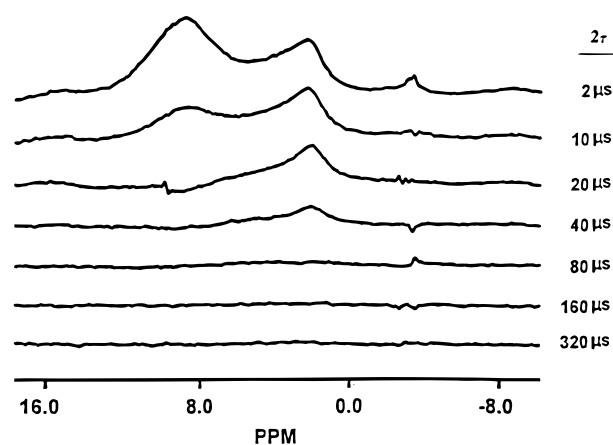


**Figure 4.**  $^1\text{H}$ – $^1\text{H}$  dipolar dephasing CRAMPS results (360 MHz) of pseudo-boehmite ( $\text{Al}_2\text{O}_3 \cdot 2.05\text{H}_2\text{O}$ ) material equilibrated at pH 6.5, followed by evacuation at 6.5 mTorr for 24 h at  $25^\circ\text{C}$ , showing dipolar dephasing time ( $2\tau$ ).

at 3.0 ppm requires  $80\ \mu\text{s}$  of dephasing to completely disappear. Dipolar dephasing preferentially attenuates the transverse magnetization of protons involved in stronger dipolar interactions with other protons.<sup>16</sup> The rapid disappearance of the proton signal at 8.2 ppm at a smaller dephasing time indicates that the protons associated with this species are involved in stronger  $^1\text{H}$ – $^1\text{H}$  dipolar coupling, probably due to hydrogen bonding, than the  $^1\text{H}$ – $^1\text{H}$  dipolar coupling exhibited by the protons resonating at 3.0 ppm. On the basis of this behavior, the 8.2 ppm resonance is assigned to closely associated, “clustered” hydroxyls, while the signal at 3.0 ppm is assigned to “isolated” hydroxyls. On the basis on the internuclear distances implied from Figure 1b, we identify the former with  $\text{Al}_2\text{OH}$  groups and the latter with  $\text{AlOH}$  groups.

Figure 5 shows the  $^1\text{H}$  CRAMPS spectra of four alumina samples dehydrated at room temperature and  $110^\circ\text{C}$ : one placed in a dessicator over Drierite at room temperature, one heated at  $110^\circ\text{C}$  at atmospheric pressure (725 Torr) for 5 h, one heated at  $110^\circ\text{C}$  at atmospheric pressure (725 Torr) for 5 h followed by evacuation at  $25^\circ\text{C}$  6.5 mTorr for 24 h, and one heated at  $110^\circ\text{C}$  under vacuum (8 mTorr) for 24 h. The  $^1\text{H}$  CRAMPS spectra of the dessicator-dried sample (Figure 5a) and the sample heated at  $110^\circ\text{C}$  under ambient pressure (Figure 5b) exhibit a broad band centered at about 4.0 ppm attributed to “physisorbed” water (*vide infra*; this material is a porous material that likely contains some internal, trapped water and “physisorbed” surface water; in addition, both interanal and extanal structural  $\text{Al}-\text{OH}$  groups are present) and a less intense shoulder at 8.2 ppm associated with the  $\text{Al}_2\text{OH}$  sites; the 3.0 ppm resonance due to  $\text{AlOH}$  sites is absent. The  $^1\text{H}$  CRAMPS spectrum corresponding to the pseudo-boehmite material that was heated at  $110^\circ\text{C}$  in ambient pressure exhibits a decreased intensity for the water proton peak (4.0 ppm) in comparison with the proton peak of the  $\text{Al}_2\text{OH}$  group, indicating that partial removal of “physisorbed” water may be achieved by simply heating the pseudo-boehmite solid at  $25^\circ\text{C}$  at  $110^\circ\text{C}$ . In their  $^1\text{H}$  NMR studies of the dehydration of the silica gel and silica–alumina surfaces, Bronnimann *et al.*<sup>16,17</sup> observed for nonevacuated samples a broad feature at ca. 3.5 ppm that was attributed to physically adsorbed water on the surfaces of silica regions and silica-like regions. On the basis of the similarity between the behavior observed for the pseudo-boehmite studied here and the  $^1\text{H}$  CRAMPS results for silica–alumina or silica materials, the broad peak at 4.0 ppm in Figure 5a and 5b is tentatively assigned to “physisorbed” water on the pseudo-boehmite alumina material. The proton signal for “physisorbed” water apparently

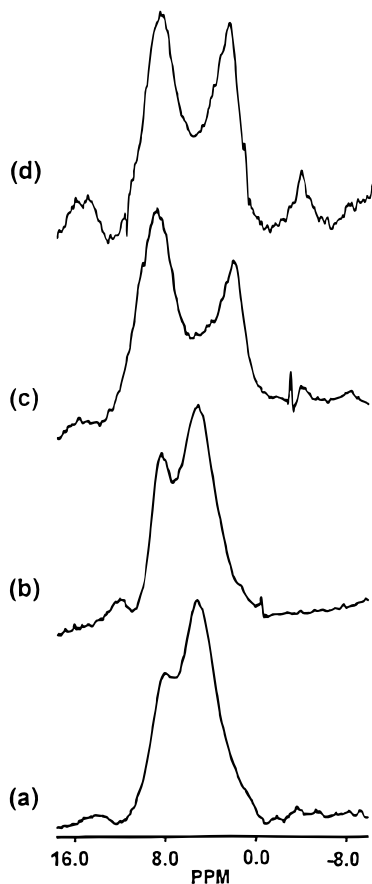


**Figure 5.**  $^1\text{H}$  CRAMPS spectra (360 MHz) of pseudo-boehmite ( $\text{Al}_2\text{O}_3 \cdot 2.05\text{H}_2\text{O}$ ) materials prepared following various dehydration procedures: (a) desiccation over Drierite at ambient pressure (725 Torr) for 72 h, (b) heating at 110 °C (in ambient pressure) for 5 h, (c) heating at 110 °C (in ambient pressure) for 5 h, followed by evacuation at 6.5 mTorr for 24 h, and (d) heating at 110 °C under vacuum (8 mTorr) for 24 h.

masks the AlOH peak at 3.0 ppm, possibly because of proton spin exchange between AlOH protons and “physisorbed” water protons; this could occur in a fashion similar to the mechanism depicted in Scheme 1 of the Huggins and Ellis model for aluminas.<sup>14</sup> The protons of “physisorbed” water molecules may also experience spin–spin flip-flop exchange with the AlOH protons on the surface, rendering the spin equilibration between the AlOH protons and “physisorbed” water protons fast, at least on the relevant time scale of these experiments.

Further water removal is achieved by heating the pseudo-boehmite solid at 110 °C followed by evacuation at 6.5 mTorr, as shown in Figure 5c. The  $^1\text{H}$  CRAMPS results show the appearance of the 3.0 ppm peak, associated with AlOH sites, and the nearly complete disappearance of the “physisorbed” water peak (4.0 ppm). The presence of spectral intensity between the 3.0 and 8.2 ppm  $^1\text{H}$  NMR signals is due to a low-intensity “physisorbed” water peak, indicating that some traces of water are still present on or within the pseudo-boehmite material; therefore, complete removal of water is not achieved utilizing this procedure. The  $^1\text{H}$  CRAMPS spectrum (Figure 7d) corresponding to a pseudo-boehmite solid that was dehydrated by heating at 110 °C in vacuo (8 mTorr) depicts only the two peaks at 8.0 and 3.0 ppm associated with surface and/or interior  $\text{Al}_2\text{OH}$  and AlOH sites, respectively, in a nearly 1:1 ratio. This result indicates that this dehydration procedure removed all the “physisorbed” water present in the pseudo-boehmite material. Thus, the  $^1\text{H}$  CRAMPS spectra of both the

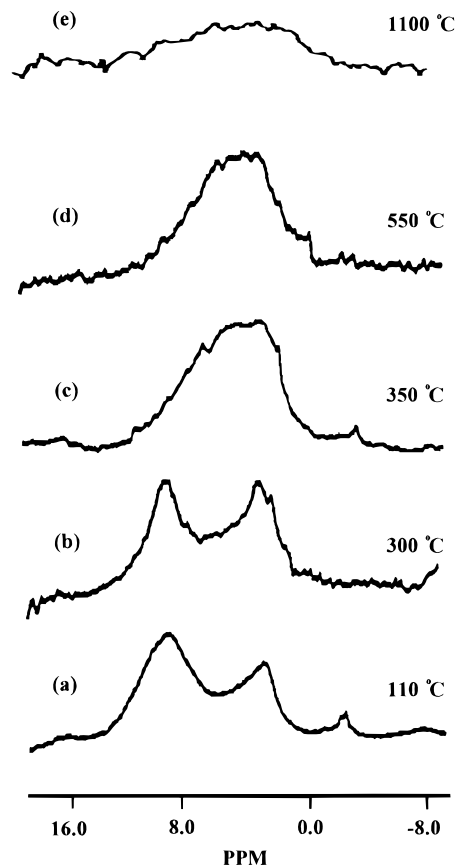


**Figure 6.**  $^1\text{H}$  CRAMPS spectra (360 MHz) of pseudo-boehmite ( $\text{Al}_2\text{O}_3 \cdot 2.05\text{H}_2\text{O}$ ) material equilibrated in aqueous suspension at pH 6.5, filtered, heated in the 110–1100 °C temperature range (as specified in the figure), followed by evacuation at 6.5 mTorr for 24 h.  $2\tau$  values of 2  $\mu\text{s}$  for all samples, except 1100 °C ( $2\tau = 0 \mu\text{s}$ ).

evacuated samples (Figure 5c,d) show that the  $\text{Al}_2\text{OH}$  (8.2 ppm) and AlOH (3.0 ppm) resonances are clearly resolved.

A series of  $^1\text{H}$  CRAMPS spectra of pseudo-boehmite samples equilibrated at pH 6.5, heated at 725 Torr over the 110–1100 °C temperature range, and then evacuated at 6.5 mTorr at 25 °C for 24 h, are given in Figure 6. The results summarized in Figure 5, as well as other  $^1\text{H}$  CRAMPS measurements not shown here, indicate that such heating/evacuation procedures with dehydration temperatures up to 350 °C remove nearly all the “physisorbed” water protons. After sample heating temperatures up to 300 °C, the peaks for both the  $\text{Al}_2\text{OH}$  and AlOH sites are observed for interior and/or surface hydroxyl groups. However, in the samples dehydrated at 725 Torr at temperatures in the 300–350 °C region, the proton peak at 8.2 ppm due to  $\text{Al}_2\text{OH}$  groups shows a drastic reduction in intensity (Figure 6b,c); this reduction in peak intensity is interpreted as due to a dehydration process as a result of condensation of adjacent, “clustered”  $\text{Al}_2\text{OH}$  surface hydroxyls. For the sample heated at 350 °C, a sharp artifact peak at about 12 ppm is also observed due to a rotor line<sup>39</sup> (Figure 6c). Further increases in the heating temperature above 350 °C result in a gradual reduction in the intensity of hydroxyl groups of the 3.0 ppm signal as a consequence of further loss of hydroxyl groups due to condensation of the “isolated” AlOH groups. However, the broad, low-intensity proton peak in the  $^1\text{H}$  CRAMPS spectra of the 550 and 1100 °C samples (Figure 6d,e) indicates that complete removal of all the Al–OH protons does not occur even after heating at 1100 °C at ambient pressure, followed by evacuation at 25 °C

(39) Fitzgerald, J. J.; Kohl, S. D.; Piedra, G.; Dec, S. F.; Maciel, G. E.; *Chem. Mater.* **1994**, *6* (11), 1915–1917

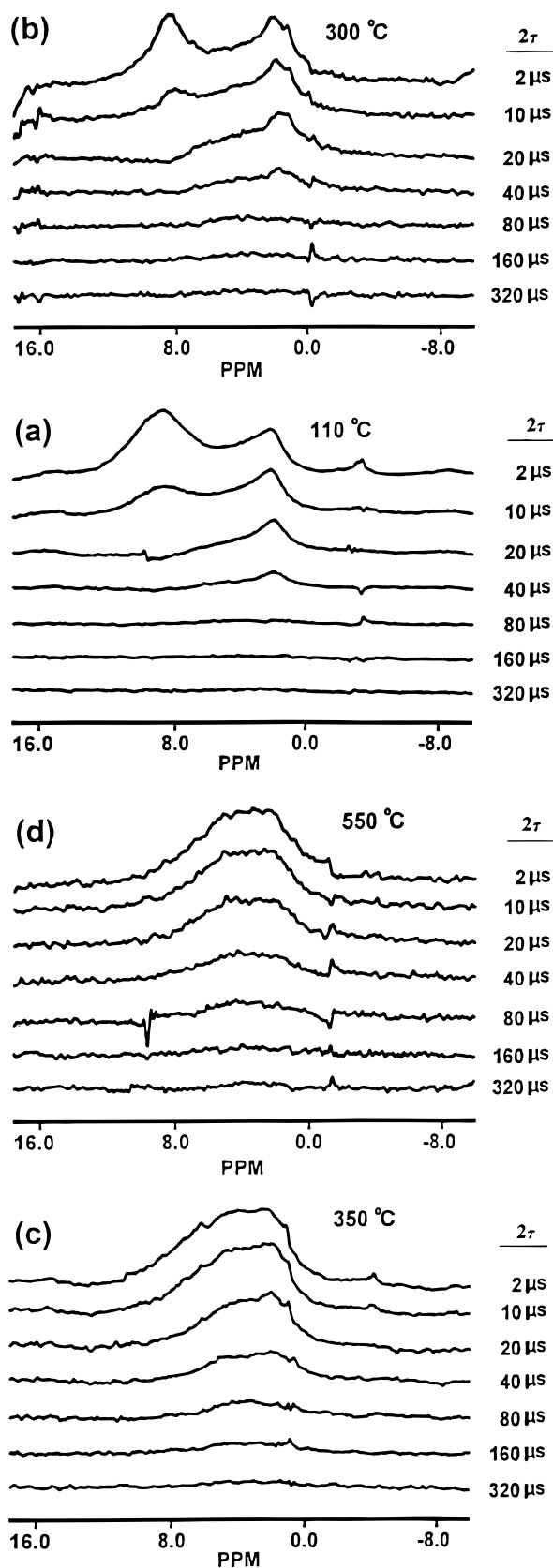


**Figure 7.**  $^1\text{H}$ – $^1\text{H}$  (360 MHz) dipolar dephasing CRAMPS results of a pseudo-boehmite ( $\text{Al}_2\text{O}_3 \cdot 2.05\text{H}_2\text{O}$ ) material equilibrated at pH 6.5, filtered, heated from 110 to 1100 °C, followed by evacuation at 6.5 mTorr for 24 h: (a) 110 °C, (b) 300 °C, (c) 350 °C, and (d) 550 °C, showing dipolar dephasing time ( $2\tau$ ).

at 6.5 mTorr for 24 h. A broad distribution of different types of residual Al–OH protons is still observed.

A series of dipolar dephasing spectra obtained on pseudo-

boehmite samples equilibrated in aqueous suspension (pH 6.5), heated at 725 Torr in the 110–550 °C temperature range, and then evacuated at 6.5 mTorr at 25 °C for 24 h, are shown in Figure 7. The dipolar dephasing spectra of the sample heated at 110 °C (Figure 7a) show two peaks at 8.2 and 3.0 ppm assigned to protons associated with the structural  $\text{Al}_2\text{OH}$  and  $\text{AlOH}$  sites, respectively. The 8.2 ppm peak dephased completely at a dephasing time of 20  $\mu\text{s}$ , whereas the 3.0 ppm peak required 80  $\mu\text{s}$  to completely disappear. The dipolar dephasing spectra (Figure 7b) of the sample heated at 725 Torr at 300 °C also show peaks due to the protons associated with the  $\text{Al}_2\text{OH}$  (8.2 ppm) and  $\text{AlOH}$  (3.0 ppm) sites, the dephasing time required to deplete these peaks (20 and 80  $\mu\text{s}$ , respectively) being the same values as obtained with the sample heated at 110 °C. The differences between the dephasing times for the 3.0 and 8.2 ppm peaks are interpreted as due to structural differences of the “clustered”  $\text{Al}_2\text{OH}$  and “isolated”  $\text{AlOH}$  groups (vide supra) but may also be explained by the differences in the proton exchange dynamics.

Figure 7c shows the series of dipolar dephasing spectra corresponding to the pseudo-boehmite sample heated at 725 Torr at temperatures up to 350 °C, followed by evacuation at 6.5 mTorr at 25 °C for 24 h. The spectra depict a broad feature centered at about 4.0 ppm, probably associated with protons of water and both internal and external structural  $\text{AlOH}$  sites, which dephases beyond observation after 320  $\mu\text{s}$  of dipolar dephasing. Figure 7d (sample heated at 550 °C, and then evacuated) also shows the same peak, although it dephases completely at 160  $\mu\text{s}$ , probably due to a lower population of protons as a result of the dehydration/dehydroxylation procedures.

The 360 MHz  $^1\text{H}$  CRAMPS spectra were obtained for “as received” pseudo-boehmite materials heated at 350 °C in ambient pressure, followed by equilibration over Drierite for 24 h, and the same material heated at 350 °C in vacuo (8 mTorr) for 24 h. The spectrum (not shown here) of the sample heated at 350 °C at ambient pressure is very similar to that shown in Figure 7c and shows a broad peak centered at 4.0 ppm due to a wide variety of protons present on the surface, including the remaining  $\text{Al}_2\text{OH}$  sites that have not condensed yet, some traces of physisorbed water, and the “isolated”  $\text{AlOH}$  sites. The simultaneous heating/evacuation procedure is more effective in eliminating the “physisorbed” water from the pseudo-boehmite material but also drastically reduces the number of structural Al–OH sites, as can be concluded from the decreased signal-to-noise ratio in the  $^1\text{H}$  CRAMPS spectrum (not shown). This in vacuo dehydration/dehydroxylation method at 350 °C completely removes both the “physisorbed” water and the majority of the  $\text{Al}_2\text{OH}$  site protons and also greatly reduces the proton population associated with the  $\text{AlOH}$  sites.

**Bulk and Surface Protons of High-Surface-Area Pseudo-boehmite.** The various dehydrated/dehydroxylated alumina materials examined in this work have been derived from a high-surface-area (230  $\text{m}^2/\text{g}$ ) pseudo-boehmite material with a chemical formula of  $\text{Al}_2\text{O}_3 \cdot 2.05\text{H}_2\text{O}$ . Calculations based on the particle size of this material (a mean diameter of 46.25  $\mu\text{m}$ ), assuming spherical geometry, indicate that about 4.2% of the total protons are within the first five  $\text{AlO}_6$  layers from the surface. Calculations based on the surface area of this material indicate that the  $\text{Al}_2\text{O}_{10}$  octahedra located in the first monolayer contain ca. 30% of the total protons, assuming a H:Al ratio of 1:1 in this monolayer. The difference between 4.2% and 30% is probably due to the porous nature of the pseudoboehmite material employed here, which contains channels or pores within the particles that are ill-defined at present. The microporous nature of this material suggests the existence of both internal

and external structural Al–OH groups for the “clustered” Al<sub>2</sub>OH and “isolated” AlOH groups.

The assignment of the <sup>1</sup>H CRAMPS resonances corresponding to the Al<sub>2</sub>OH and AlOH sites have been based on the assumption that these “aluminol” groups are present both on the surface (external) and within (internal) the pseudo-boehmite material and are structurally similar to the Al<sub>2</sub>OH and AlOH sites of crystalline boehmite.<sup>21–24</sup> According to this model, the pseudo-boehmite structure consists of three different types of “aluminol” groups: (a) interlayer Al<sub>2</sub>OH sites, (b) “clustered” Al<sub>2</sub>OH surface and/or internal sites, and (c) surface and/or internal AlOH sites. Interlayer and “clustered” Al<sub>2</sub>OH sites differ in the nature of their hydrogen bonding. In the interlayer Al<sub>2</sub>OH sites, the hydrogen bonding occurs between the oxygen of one layer and the hydrogen of an adjacent layer, whereas in the “clustered” Al<sub>2</sub>OH groups, the hydrogen bond is formed between an oxygen atom and a hydrogen atom coordinated to an adjacent oxygen in the same layer. The dipolar dephasing results indicate stronger <sup>1</sup>H–<sup>1</sup>H dipolar interactions of the Al<sub>2</sub>OH protons, which suggest the existence of strong hydrogen bonding; however, the dipolar dephasing data do not provide enough evidence to make a clear distinction between the two types of Al<sub>2</sub>OH sites. In the AlOH groups, each oxygen is only 2-coordinate, with available electron pairs that might be utilized in the formation of hydrogen bonds with neighboring water molecules. This latter situation would account for the proton exchange process between AlOH groups and water molecules.

There are three possible combinations of hydroxyl sites by which condensation might occur: (1) the combination of pairs of Al<sub>2</sub>OH sites, (2) the combination of pairs of AlOH sites, and (3) the combination of Al<sub>2</sub>OH sites with AlOH sites. The reported internuclear O–O distance between a pair of octahedral, edge-sharing Al<sub>2</sub>OH sites in crystalline boehmite is 2.535 Å, the same as the O–O distance between a pair of AlOH sites; the corresponding O–O distance within a Al<sub>2</sub>OH–AlOH pair is 2.558 Å, whereas the distance within the interlayered Al<sub>2</sub>OH–Al<sub>2</sub>OH pair is 2.709 Å.<sup>4,21–24</sup> On the basis of these parameters, Al<sub>2</sub>OH–Al<sub>2</sub>OH condensation and AlOH–AlOH condensation between octahedral sites are expected to be favored over the condensation of Al<sub>2</sub>OH–AlOH pairs and should definitely be preferred over the condensation of interlayered Al<sub>2</sub>OH pairs. Figure 8a depicts a proposed scheme by which the condensation of axially distributed surface/internal AlOH groups (oriented along the *a* axis) may occur. The condensation of such axial AlOH groups would result in the formation of some highly distorted, “external” 6-coordinate AlO<sub>4</sub>(OH)<sub>2</sub> sites and “internal” 6-coordinate AlO<sub>4</sub>(OH)<sub>2</sub> sites. The condensation of equatorial Al<sub>2</sub>OH sites (located on the *b*–*c* plane) would give rise to some “external” 5-coordinate AlO<sub>4</sub>OH sites and “internal” 5-coordinate AlO<sub>5</sub> sites, as shown in Figure 8b. Condensation of the interlayer Al<sub>2</sub>OH groups results in cross-linking of adjacent layers with concomitant formation of channels or pores throughout the material, as depicted in Figure 8c, where highly distorted, 6-coordinate AlO<sub>6</sub> sites are generated. The simultaneous condensation of AlOH and Al<sub>2</sub>OH groups, which would occur by a simultaneous combination of the schemes described in Figure 8a,b, would also generate highly distorted, 4-coordinate AlO<sub>4</sub> sites (not shown here).

On the basis of the nature of the species formed following the condensation of the two different types of structural “aluminol” sites (both internal and external), one could envision that the formation of the less-distorted 5-coordinated AlO<sub>4</sub>OH sites should be favored over the formation of the more distorted 6-coordinated AlO<sub>4</sub>(OH)<sub>2</sub> sites. Hence, it seems reasonable to propose that the condensation of equatorial Al<sub>2</sub>OH sites will

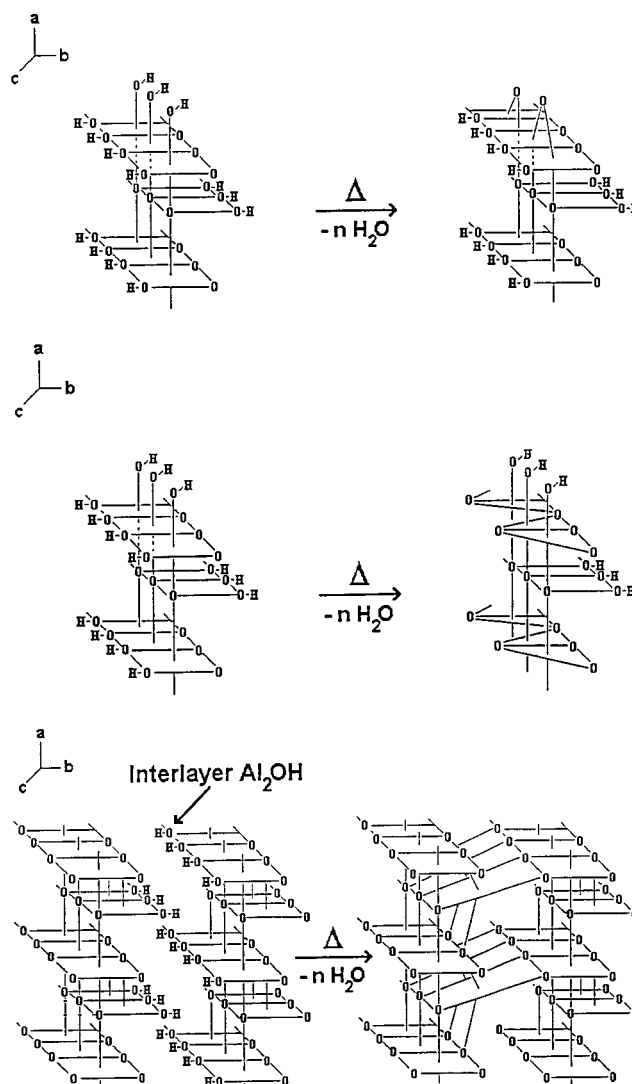


**Figure 8.** Proposed schemes for the condensation of structural hydroxyl groups of pseudo-boehmite: (a) condensation of “isolated” AlOH groups, (b) condensation of “clustered” Al<sub>2</sub>OH groups, (c) condensation of interlayered Al<sub>2</sub>OH groups. Some of the Al–O bonds were deliberately omitted in the figure for clarity.

be energetically more favorable than the condensation of axially distributed AlOH hydroxyl groups. Structurally, the order in which the different “aluminol” groups condense upon heating may be predicted to be the following: first, the equatorial, “clustered” Al<sub>2</sub>OH sites, second, the axial, “isolated” AlOH sites, and third, the interlayer Al<sub>2</sub>OH sites.

**MAS <sup>27</sup>Al NMR Studies of the Dehydration of High-Surface-Area (HSA) Pseudo-boehmite.** MAS <sup>27</sup>Al NMR studies of the dehydration products of bayerite, boehmite, sodium aluminate dihydrate, Na<sub>2</sub>O·Al<sub>2</sub>O<sub>3</sub>·3H<sub>2</sub>O, and the minerals pyrophyllite and kaolinite have been successfully used to determine and assign different 4-, 5-, and 6-coordinate aluminum sites that occur in these materials during their dehydration in the solid state.<sup>26–29</sup> In the 14 T <sup>27</sup>Al NMR work described herein for the dehydration products of the pseudo-boehmite materials produced over the temperature range 110–1100 °C, structural information regarding changes in the coordination environments of aluminum sites in these materials has been obtained. The relationship between these aluminum site changes and the observed proton population changes that occur in these dehydrated materials as identified from the <sup>1</sup>H CRAMPS results are also discussed.

A series of 156.38 MHz <sup>27</sup>Al NMR spectra of the pseudo-



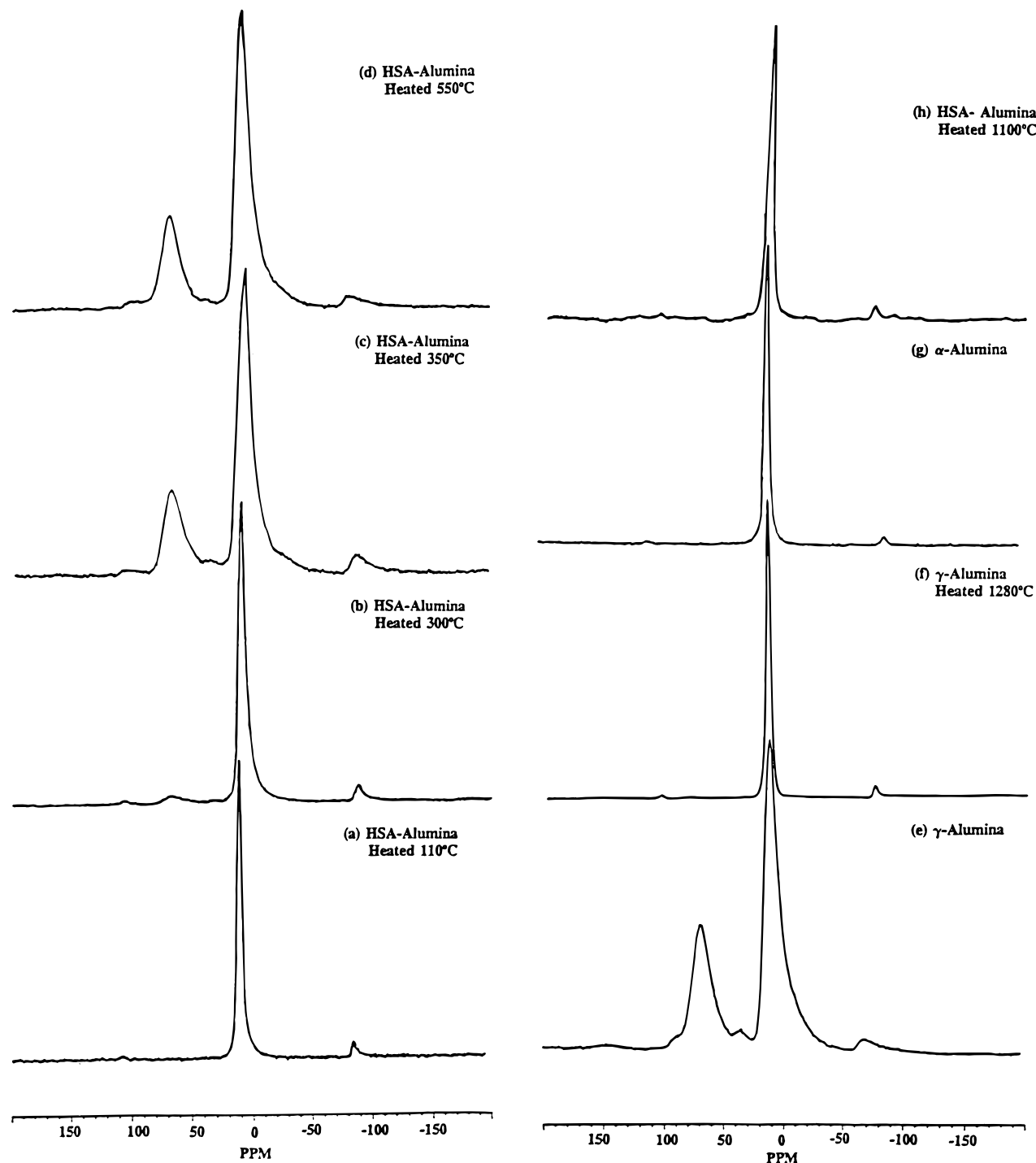


**Figure 9.**  $^{27}\text{Al}$  MAS NMR spectra (14 T) of various aluminum oxide materials: (a) pseudo-boehmite heated at 110 °C, (b) pseudo-boehmite heated at 300 °C, (c) pseudo-boehmite heated at 350 °C, (d) pseudo-boehmite heated at 550 °C, (e)  $\gamma$ -alumina, (f)  $\gamma$ -alumina, heated 3 h at 1280 °C, (g)  $\alpha$ -alumina, (h) pseudo-boehmite heated 1100 °C.

boehmite material and its dehydration products obtained over the temperature range 110–1100 °C at ambient pressure, followed by evacuation at 6.5 mTorr at 25 °C for 24 h, are given in Figure 9, together with various reference spectra of  $\alpha$ - $\text{Al}_2\text{O}_3$ ,  $\gamma$ - $\text{Al}_2\text{O}_3$  and  $\gamma$ - $\text{Al}_2\text{O}_3$  dehydrated at ambient pressure at 1280 °C, followed by similar room temperature evacuation procedures. The series of pseudo-boehmite materials are identical with those samples used to obtain the dehydration profile shown in Figure 2A and to obtain the  $^1\text{H}$  CRAMPS NMR results shown in Figures 6 and 7. The  $^{27}\text{Al}$  NMR spectrum (Figure 9a) of pseudo-boehmite dehydrated at 110 °C, followed by evacuation, exhibits a sharp peak at 8.8 ppm similar to that of the “as received” material, which is assigned to  $\text{AlO}_6$  sites

and is similar to the  $^{27}\text{Al}$  NMR peak observed for crystalline boehmite and diaspore (spectra not shown here). In the material produced at a dehydration temperature of 300 °C at ambient pressure, followed by evacuation at 25 °C at 6.5 mTorr, the  $^{27}\text{Al}$  NMR spectrum (Figure 9b) shows a low-intensity peak at 69 ppm due to newly formed 4-coordinate  $\text{AlO}_4$  sites, in addition to the 6-coordinate peak at 8.8 ppm. Dehydration at ambient pressure at 350 °C, followed by evacuation at 6.5 mTorr at 25 °C for 24 h, produces an  $^{27}\text{Al}$  NMR spectrum (Figure 9c) that shows three peaks, a more intense 4-coordinate peak at 67.8 ppm, a broad but intense peak at 9.0 ppm due to 6-coordinate aluminum, and a weak but discernible NMR signal at 37.0 ppm that is assigned to 5-coordinate aluminum sites. The  $^{27}\text{Al}$  NMR

spectrum of the 350 °C sample is similar to the spectrum of a commercial  $\gamma$ -alumina sample (Figure 9e, peaks at 9.0 and 68.8 ppm), indicating that the pseudo-boehmite material is dehydrated to a transition alumina.

The spectrum (Figure 9c) of the sample dehydrated at ambient pressure at 550 °C, followed by room temperature evacuation at 6.5 mTorr for 24 h, is very similar to that of the sample dehydrated at 725 Torr at 350 °C, showing the same three resonances at 9.0, 36.5, and 68.4 ppm. The three spectra of the samples dehydrated at 725 Torr at 300, 350, and 550 °C given in Figure 9 all show the presence of this 36–37 ppm aluminum peak. This  $^{27}\text{Al}$  NMR peak in the chemical shift range 36–37 ppm observed in these spectra of the dehydrated samples is thus assigned to 5-coordinate  $\text{AlO}_5$  sites, consistent with similar assignments of 5-coordinate  $\text{AlO}_5$  sites observed in the  $^{27}\text{Al}$  NMR of barium aluminum glycolate, andalusite, pyrophyllite dehydroxylate, dehydrated kaolinite (metakaolinite), and selected silica–alumina solids.<sup>28–30</sup> The reference  $^{27}\text{Al}$  NMR spectrum (Figure 9e) of the commercial  $\gamma$ -alumina also shows these three NMR peaks, which are consistent with these assignments for the products of pseudo-boehmite dehydration at intermediate temperatures (Figure 9b–d).

At a higher temperature of ambient pressure dehydration, 1100 °C (followed by similar room temperature evacuation), the  $^{27}\text{Al}$  NMR spectrum of the dehydrated pseudo-boehmite material shows only a single 6-coordinate  $\text{AlO}_6$  resonance at 14.3 ppm (Figure 9h), similar to that in the spectra of  $\alpha$ -alumina (Figure 9g, 13.9 ppm) and the  $\gamma$ -alumina sample (Figure 9f, 14.1 ppm) that has been heated at 1280 °C at ambient pressure. These results provide conclusive evidence that the transition aluminas produced from the pseudo-boehmite material by heating at ambient pressure in the 300–350 °C temperature range (followed by room temperature evacuation) undergo a solid-state thermal conversion to  $\alpha$ -alumina at 1100 °C, similar to the  $\alpha$ - to  $\gamma$ -alumina conversion observed for the commercial  $\gamma$ - $\text{Al}_2\text{O}_3$  material.<sup>26</sup>

A fundamental question regarding the  $^{27}\text{Al}$  NMR spectra is whether these spectra show intensities that properly represent the amounts of aluminum in the dehydrated samples. This is particularly true for  $^{27}\text{Al}$  NMR signals associated with aluminum sites with very low symmetry and, consequently, very large electric field gradients that produce broad NMR resonances. The question of “invisible aluminum” has been a common problem noted in the literature for solid-state  $^{27}\text{Al}$  NMR studies of minerals such as andalusite and dehydrated clays such as pyrophyllite dehydroxylate and metakaolin,<sup>28–32</sup> and surface aluminum sites on transition aluminas that have reduced coordination numbers less than 6.<sup>13,14,26,34–36</sup> To address this significant question, spin counting experiments were carried out on the pseudo-boehmite material and its dehydration products formed over the temperature range 300–1280 °C. A plot of the integrated  $^{27}\text{Al}$  NMR centerband intensity for pseudo-boehmite and its dehydrated products as a function of pulse length (0.10–1.0  $\mu\text{s}$ ), shows a complex relationship (related to the relative size of the quadrupolar interactions and the rf field strength).<sup>35–37</sup> Comparison to the integrated signal for the centerband of an authentic sample of kaolin (containing a known number of  $^{27}\text{Al}$  spins) gave the NMR-detectable aluminum content of each of the dehydrated materials. The integrated intensities after a 0.10  $\mu\text{s}$  pulse (the shortest achievable with the available spectrometer hardware and software) are shown by comparison to the TGA results (Table 2) to be proportional to the number of Al spins in the sample. (Uncertainties were estimated by repeat analysis and are dominated by the uncertainty in the determination of sample mass (the samples ranged

**Table 2.** Summary of  $^{27}\text{Al}$  Spin Counting Experiments Based on NMR and TGA Measurements for Pseudo-Boehmite Samples Heated at the Temperatures Noted

dehydration temp (°C)	sample wt (mg $\pm$ 0.1 mg)	%Al by NMR	%Al by TGA
110	10.1	44 $\pm$ 2%	42%
300	5.3	45 $\pm$ 2%	46%
350	4.7	51 $\pm$ 3%	48%
550	7.7	52 $\pm$ 2%	51%
1100	13.6	53 $\pm$ 1%	52%
1280	12.3	53 $\pm$ 1%	54%

from 4 to 14 mg), with an uncertainty of  $\pm 0.1$  mg; hence, the smallest samples show largest uncertainties.) Comparison of the aluminum content determined by  $^{27}\text{Al}$  NMR spin counting to the values obtained from TGA analysis (Table 2) indicates that (to within experimental uncertainty) all of the aluminum nuclei in the dehydrated materials are being observed at very short pulse lengths at 14 T magnetic field strength. Therefore, the major changes in the  $^{27}\text{Al}$  NMR spectra of the dehydrated transition aluminas obtained by calcination of pseudo-boehmite in this study indicate that all of the aluminas are NMR observable and that the integrated peak intensities accurately reflect the 4-, 5-, and 6-coordinate aluminum compositions in these samples. These results may be contrasted with the only work reported on the relative contents of 4- and 6-coordinate aluminas in transition aluminas by John et al.,<sup>26</sup> where not all of the aluminum is observable under the conditions used in those early studies.

**Relationship between  $^1\text{H}$  and  $^{27}\text{Al}$  NMR Results.** The major changes in the aluminum coordination environment displayed in the  $^{27}\text{Al}$  NMR results of the dehydration products of the HSA pseudo-boehmite material may be interpreted in relation to the information obtained on the proton populations of these same dehydrated materials from the  $^1\text{H}$  CRAMPS results. In the sample dehydrated at ambient pressure at 110 °C, followed by room temperature evacuation, the  $^{27}\text{Al}$  NMR shows a single 6-coordinate peak at 8.8 ppm due to  $\text{Al}(\text{OH})_6$  sites, while the  $^1\text{H}$  CRAMPS spectrum of a sample heated at 110 °C under vacuum (6.5 mTorr) for 24 h shows two resonances due to the “isolated”  $\text{AlOH}$  (2.3 ppm) and “clustered”  $\text{Al}_2\text{OH}$  (8.2 ppm) groups, indicating that the disordered pseudo-boehmite structure is intact following these treatments. Upon heating the pseudo-boehmite material up to 300 °C, followed by evacuation, its  $^{27}\text{Al}$  NMR spectrum exhibits a single, intense 8.8 ppm resonance, with the appearance of very low signal intensity in the 4- and 5-coordinate Al chemical shift region (30–70 ppm), indicating the initial stages of the condensation of Al–OH groups. The  $^1\text{H}$  CRAMPS spectrum of this sample shows that the resonances due to the two  $\text{AlOH}$  and  $\text{Al}_2\text{OH}$  proton populations are virtually unchanged in comparison with those of the sample heated at ambient pressure at 110 °C (followed by room temperature evacuation), except for the appearance of a low-intensity, broad signal between these two peaks (Figure 6b), possibly due to residual “physisorbed” water protons. Proton signals due to OH groups coordinated on aluminas in both the samples dehydrated at 110 and 300 °C, followed by evacuation at 6.5 mTorr, are not obscured by this weak proton peak at 4.0 ppm due to “physisorbed” water. It is proposed on the basis of the  $^1\text{H}$  CRAMPS spectrum of the sample dehydrated at 300 °C under ambient pressure, and the subsequent changes in the spectra of the samples dehydrated at 350 and 550 °C under ambient pressure, to be described below, that these early stages of condensation of aluminum-coordinated hydroxyl groups probably occur in the absence of “physisorbed” water and that the loss of water at 300 °C is principally due to

the initiation of condensation of adjacent hydroxyl groups associated with the "clustered"  $\text{Al}_2\text{OH}$  groups of the pseudo-boehmite material.

The  $^{27}\text{Al}$  NMR spectra (Figure 9c,d) of the samples dehydrated at 350 and 550 °C under ambient pressure, followed by room temperature evacuation at 6.5 mTorr for 24 h, show 4-, 5-, and 6-coordinate peaks with fractional areas of 0.23, 0.03, and 0.74, respectively. The fractional peak areas for the 4-, 5-, and 6-coordinate aluminum peaks in the spectrum of  $\gamma$ -alumina (Figure 9e) are 0.27, 0.04, and 0.69. John, Alma, and Hays<sup>26</sup> have reported 11.4 T  $^{27}\text{Al}$  NMR results which show that the various transition aluminas have the following fractional peak areas for the 4-coordinate aluminums,  $\gamma$  (0.25),  $\delta$  (0.25),  $\theta$  (0.00), and  $\eta$  (0.35), with the remaining peak areas being due to 6-coordinate aluminums. The works of John et al.<sup>26</sup> and Lippens<sup>33</sup> have also shown that crystalline boehmite undergoes dehydration to  $\gamma$ -alumina (0.27  $T_d$ ) at 450 °C, then to  $\delta$ -alumina (0.25  $T_d$ ) at 750 °C, then to a mixture of  $\alpha$ - and  $\theta$ -alumina (both 0.00  $T_d$ ) at 1000 °C, and finally to  $\alpha$ -alumina (0.00  $T_d$ ) at 1200 °C. The  $^{27}\text{Al}$  NMR results obtained here for the pseudo-boehmite material substantiate the view that the formation of either  $\gamma$ - or  $\delta$ -alumina begins initially at 300 °C and is essentially complete, from a  $^{27}\text{Al}$  NMR viewpoint, in the 350–550 °C temperature range, where a fractional 4-coordinate composition in the range 0.25–0.27 is observed.

The  $^1\text{H}$  CRAMPS results provide additional insight into the formation of transition alumina (either  $\gamma$  or  $\delta$ ) in the 350–550 °C temperature region from the high-surface-area pseudo-boehmite. The formation of principally 4-coordinate and 6-coordinate aluminums, in addition to a minor population of 5-coordinate aluminums, occurs by condensation of both the "clustered"  $\text{Al}_2\text{OH}$  and "isolated"  $\text{AlOH}$  groups in the 350–550 °C temperature region. The rate of condensation of the "clustered"  $\text{Al}_2\text{OH}$  groups is greater than that of the "isolated"  $\text{AlOH}$  groups and occurs at lower temperature, as evidenced by the more significant changes in the 8.2 ppm peak in the  $^1\text{H}$  CRAMPS spectrum for the lower temperature (350 °C) sample (Figure 6c) in comparison with the spectrum of the sample dehydrated at 550 °C (Figure 6d). The various schemes for the condensation of the  $\text{AlOH}$  groups, as shown in Figure 8, indicate that the adjacent "clustered"  $\text{Al}_2\text{OH}$  groups may condense to 5-coordinate aluminums, with the formation of distorted 6-coordinate sites as well. Simultaneous condensation of  $\text{Al}_2\text{OH}$  and  $\text{AlOH}$  groups would lead to the formation of appreciable amounts of distorted, 4-coordinate aluminums, as is observed from the  $^{27}\text{Al}$  NMR spectra of the samples dehydrated at 350 and 550 °C at ambient pressure, followed by room temperature evacuation at 6.5 mTorr for 24 h. The presence of a low population of 5-coordinate aluminums in these spectra suggest that the  $\text{AlO}_5$  species is a likely intermediate formed prior to the formation of the more abundant 4-coordinate aluminums.

In the samples dehydrated in the 550–1100 °C temperature range, the  $^1\text{H}$  CRAMPS spectra show a very broad resonance extending over approximately a 10 ppm chemical shift range. However, the relative proton populations of the sample dehy-

drated at 1100 °C, followed by evacuation, are markedly reduced relative to the spectrum of the sample dehydrated at 550 °C, as evidenced by the observed decrease in the signal-to-noise ratio of the  $^1\text{H}$  CRAMPS signal for the sample dehydrated at 1100 °C. The observed broad proton peaks in the spectra of both the samples dehydrated at 550 and 1100 °C at ambient pressure, followed by room temperature evacuation, are likely a result of a wide range of chemically different hydrogen-bearing  $\text{AlO}_4$  and  $\text{AlO}_6$  aluminum polyhedra in the 550 °C sample and a similar wide distribution of  $\text{AlO}_6$  octahedra for the sample dehydrated at 1100 °C. Another possible contribution to the broadened  $^1\text{H}$  CRAMPS resonances is the occurrence of "proton hopping", as proposed by Huggins and Ellis,<sup>14</sup> from their variable-temperature  $^{27}\text{Al}$  NMR studies of partially or fully dehydrated transition aluminas.

## Conclusions

The  $^1\text{H}$  CRAMPS results and weight-loss data indicate that most of the "physisorbed" water protons are lost at 110 °C (with or without evacuation). In addition, the  $^1\text{H}$  CRAMPS results and weight-loss data indicate that water protons from aluminum-coordinated hydroxyls in the "clustered"  $\text{Al}_2\text{OH}$  sites are removed from the pseudo-boehmite material at temperatures in the 200–350 °C range, whereas protons from aluminum-coordinated hydroxyls in the "isolated"  $\text{AlOH}$  sites begin to condense at higher temperatures (350–1100 °C). The favored condensation of "clustered"  $\text{Al}_2\text{OH}$  groups over the condensation of the "isolated"  $\text{AlOH}$  groups is presumably associated with the less distorted nature of the 5-coordinated  $\text{AlO}_4\text{OH}$  species that is formed by such processes and/or the relative proximity of the "clustered"  $\text{Al}_2\text{OH}$  groups to one another. In the case of the formation of a "less" distorted  $\text{AlO}_4\text{OH}$  species or the proximity of  $\text{Al}_2\text{OH}$  groups to one another, the condensation of these surface Brönsted acid sites gives rise to the formation of strained Al–O–Al linkages throughout the alumina surface as a result of oxygen vacancies (5-coordinate Al) or oxygen defects (distorted 6-coordinate Al). The  $^{27}\text{Al}$  NMR evidence shows the appearance of minor 5-coordinate species in addition to an approximately 3:1 ratio of hydrogen-bearing 6-coordinate/4-coordinate aluminum oxyhydroxide species distribution present in a  $\gamma$ - or  $\delta$ -transition alumina material formed following dehydration of the pseudo-boehmite material in the 350–550 °C range at ambient pressure (followed by room temperature evacuation at 6.5 mTorr). With a heating temperature of 1100 °C, followed by evacuation, dehydration of the proton-bearing  $\gamma$ - or  $\delta$ -transition alumina to  $\alpha$ -alumina containing  $\text{AlO}_6$  structural moieties with a very low hydrogen content occurs.

**Acknowledgment.** The authors gratefully acknowledge support from the National Science Foundation Grants No. RII-8902066 and CHE-9021003 and the technical assistance of Dr. Bruce Hawkins, Dr. Herman Lock and Dr. Mark F. Davis of the Colorado State University NMR Center, Fort Collins, CO. J.J.F. acknowledges support of the Office of the President, South Dakota State University.

JA970788U